

SCHRÖMIND: MITIGATING HALLUCINATIONS IN MULTIMODAL LARGE LANGUAGE MODELS VIA SOLVING THE SCHRÖDINGER BRIDGE PROBLEM

Ziqiang Shi*, Ruijie Liu*, Shanshan Yu†, Satoshi Munakata†, Koichi Shirahata†

* Fujitsu Research & Development Center Co., LTD., Beijing, China

† Fujitsu Limited, Tokyo, Japan

ABSTRACT

Recent advancements in Multimodal Large Language Models (MLLMs) have achieved significant success across various domains. However, their use in high-stakes fields like health care remains limited due to persistent hallucinations, where generated text contradicts or ignores visual input. We contend that MLLMs can comprehend images but struggle to produce accurate token sequences. Minor perturbations can shift attention from truthful to untruthful states, and the autoregressive nature of text generation often prevents error correction. To address this, we propose SchröMind—a novel framework reducing hallucinations via solving the Schrödinger bridge problem. It establishes a token-level mapping between hallucinatory and truthful activations with minimal transport cost through lightweight training, while preserving the model’s original capabilities. Extensive experiments on the POPE and MME benchmarks demonstrate the superiority of SchröMind, which achieves state-of-the-art performance while introducing only minimal computational overhead.

Index Terms— Multimodal large language models, hallucination mitigation, Schrödinger bridge problem, entropy-regularized optimal transport, attention activation steering

1. INTRODUCTION

Multimodal Large Language Models (MLLMs) excel at processing visual and textual information, advancing tasks such as visual question answering (VQA), image captioning, and visual reasoning [1, 2, 3]. However, they frequently suffer from object hallucination, where textual descriptions contradict the image content [4, 5, 6, 7]. This stems from an over-reliance on unimodal priors (e.g., linguistic biases) during inference, posing significant risks in safety-critical domains like medical diagnosis and autonomous driving.

Existing mitigation strategies often incorporate external knowledge or fine-tune on additional annotated data, but require substantial computational resources [8, 9, 10]. More recent decoding-time interventions, such as contrastive decoding [4, 11, 12], suppress hallucinations without retraining, yet may compromise fluency and increase latency. Lightweight

inference-time methods that adjust activations without updating parameters—known as *activation engineering* [13, 14]—are thus gaining attention. Such methods often use contrastive samples to derive steering vectors that alter model behavior. For instance, ITI [13] successfully reduces hallucination in large language models (LLMs) by injecting steering activation vectors into attention layers. Subsequent work extended these ideas to MLLMs, leading to methods like ICT [14], which operate at global and local visual levels and enhance cross-modal alignment.

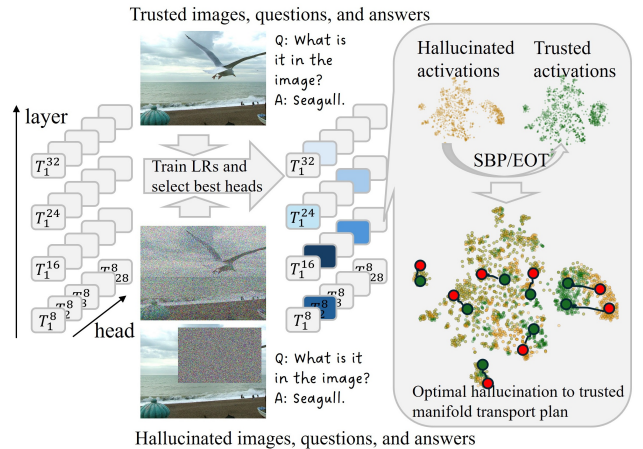


Fig. 1: Schematic of SchröMind. MLLMs process correct and hallucinated responses to extract attention activations. Classifiers then identify critical attention heads and analyze token wise influences. SBP/EOT learns a distribution mapping to mitigate hallucinations.

But most current intervention techniques apply a uniform steering direction across all tokens in an attention head, implicitly assuming that shifting the hallucinatory activation manifold yields the truthful manifold [13, 14]. We argue that this view is oversimplified—each token’s activation lies at a unique position, requiring personalized intervention. To this end, we propose SCHRÖMIND, which models the hallucination and truthful manifolds jointly and derives token-specific intervention directions via solving the Schrödinger bridge

problem (SBP) [15]. This optimal transport-based approach ensures minimal-cost mapping between manifolds, enabling precise correction with little training and plug-and-play deployment.

SchröMind’s contributions are threefold: 1) We propose a personalized intervention framework that formulates activation correction as an optimal transport problem between hallucination and truthful manifolds. 2) SchröMind is the first to use a Schrödinger bridge-based method for token-level intervention, requiring only minutes of training and allowing immediate application. 3) Extensive experiments show that SchröMind outperforms previous state-of-the-art (SOTA) methods across multiple benchmarks.

2. SCHRÖMIND

2.1. Preliminaries and Notation

While MLLMs’ vision encoders capture sufficient image details, strong language priors in the LLM module can induce object hallucinations [5, 6]. To address this, we adjust intermediate Transformer states toward higher reliability. The K -layer Transformer is formalized as:

$$\mathbf{x}^{(k)} = \mathbf{x}^{(k-1)} + \sum_{m=1}^M \mathcal{T}_m^{k-1}(\mathbf{x}^{(k-1)}) \Theta_m^{k-1}, \quad (1)$$

where M denotes attention heads per layer, $\mathcal{T}_m^{k-1}(\cdot)$ computes attention-weighted features for head m at layer $k-1$, and $\Theta_m^{k-1} \in \mathbb{R}^{D \times DM}$ projects outputs to the D -dimensional representation space. The final layer transforms $\mathbf{x}^{(K)}$ into vocabulary logits, yielding the token prediction distribution:

$$P(y_t | \mathbf{y}_{1:t-1}) = \sigma(\mathcal{L}(\mathbf{x}_t^{(K)})),$$

with $\mathbf{y}_{1:t-1}$ as the prior token sequence.

As shown in Fig. 1, we define the hallucinated attention distribution $\mathbb{P}_{\text{hallu}} \in \mathcal{P}(\mathbb{R}^D)$ as activations induced by hallucinated content due to degraded visual inputs, language priors or ignoring vision tokens, whereas the factual distribution $\mathbb{P}_{\text{fact}} \in \mathcal{P}(\mathbb{R}^D)$ corresponds to authentic visual inputs. SchröMind mitigates hallucinations by correcting $\mathbb{P}_{\text{hallu}}$ toward \mathbb{P}_{fact} via solving SBP, preserving semantic coherence while aligning distributions through Schrödinger bridge theory.

2.2. Defining Hallucination Mitigation in SchröMind

We construct a mapping transforming hallucinated activations $\mathbb{P}_{\text{hallu}}$ into trustworthy activations \mathbb{P}_{fact} using SBP [15] and its static extension, the entropy-regularized optimal transport (EOT) [16]. The SBP/EOT formulation minimizes transport

cost with entropy regularization:

$$\min_{\pi \in \Pi(\mathbb{P}_{\text{hallu}}, \mathbb{P}_{\text{fact}})} \iint \frac{1}{2} \|\mathbf{a}_{\text{hallu}} - \mathbf{a}_{\text{fact}}\|^2 d\pi + \epsilon \text{KL}(\pi || \mathbb{P}_{\text{hallu}} \times \mathbb{P}_{\text{fact}}), \quad (2)$$

where Π denotes valid joint distribution between hallucination and reliable attention activation, the quadratic term measures activation dissimilarity, and $\epsilon > 0$ regularizes for stability. The optimal plan π^* defines a probabilistic correction from hallucinated to factual activations.

While π^* provides the optimal static mapping, it lacks temporal dynamics. We therefore introduce a time dimension $t \in [0, 1]$ with $t = 0$ and $t = 1$ corresponding to $\mathbb{P}_{\text{hallu}}$ and \mathbb{P}_{fact} , respectively. Using a Wiener process \mathbb{W}^{ϵ} with diffusion coefficient $\sqrt{\epsilon}$ as prior, the SBP/EOT yields a diffusion process governed by:

$$d\mathbf{a}_t = \mathbf{g}^*(\mathbf{a}_t, t) dt + \sqrt{\epsilon} d\mathbf{W}_t, \quad (3)$$

where the optimal drift \mathbf{g}^* steers activations away from hallucinatory modes, as shown in Fig. 2.

The EOT-SBP equivalence establishes marginal consistency ($\pi^{\mathbb{T}^*} = \pi^*$) and reveals intermediate paths as Brownian bridges. This duality enables two mitigation strategies: static correction via π^* for instantaneous remapping, and dynamic intervention using $\mathbf{g}^*(\mathbf{a}, t)$ for progressive adjustment during inference.

2.3. Hallucination-to-Truth Manifold Mapping

The SBP/EOT solution to Eq. (2) admits a closed form [15, 16]:

$$\pi^*(\mathbf{a}_0, \mathbf{a}_1) = u^*(\mathbf{a}_0) \exp(\langle \mathbf{a}_0, \mathbf{a}_1 \rangle / \epsilon) v^*(\mathbf{a}_1), \quad (4)$$

where $\mathbf{a}_0 \equiv \mathbb{P}_{\text{hallu}}$, $\mathbf{a}_1 \equiv \mathbb{P}_{\text{fact}}$, and u^* , v^* incorporate hallucination and reliable Schrödinger potentials. This yields the conditional distribution $\pi^*(\mathbf{a}_1 | \mathbf{a}_0) \propto \exp(\langle \mathbf{a}_0, \mathbf{a}_1 \rangle / \epsilon) v^*(\mathbf{a}_1)$ for transforming hallucinated activations. The correction path is governed by:

$$g^*(\mathbf{a}, t) = \epsilon \nabla_{\mathbf{a}} \log \int \mathcal{N}(\mathbf{a}' | \mathbf{a}, (1-t)\epsilon \mathbf{I}) \phi^*(\mathbf{a}') d\mathbf{a}', \quad (5)$$

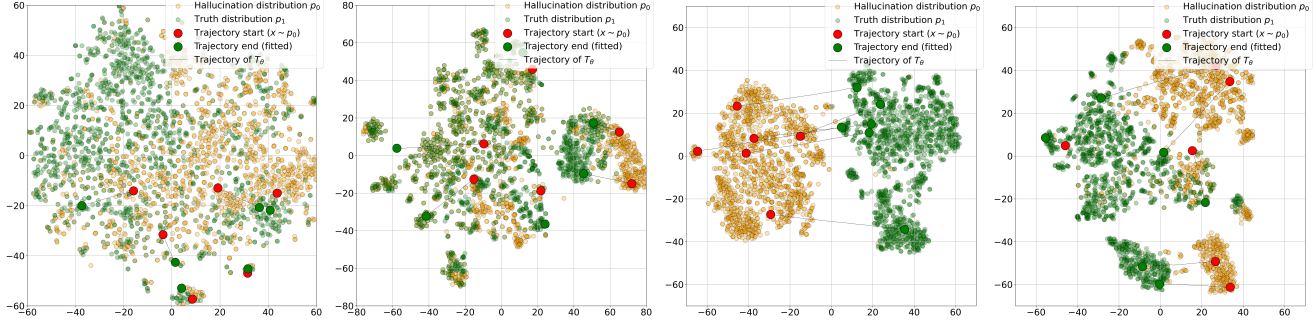
defining a smooth transport field that avoids semantic discontinuities.

Inspired by Korotin et al. [16], we approximate trustworthy potential v^* via Gaussian mixtures:

$$v_{\theta}(\mathbf{a}_1) = \sum_{i=1}^G \alpha_i \mathcal{N}(\mathbf{a}_1 | r_i, \epsilon S_i), \quad (6)$$

with learnable $\theta = \{\alpha_i, r_i, S_i\}$. The conditional distribution becomes:

$$\pi_{\theta}(\mathbf{a}_1 | \mathbf{a}_0) = \frac{1}{c_{\theta}(\mathbf{a}_0)} \sum_{i=1}^G \alpha_i(\mathbf{a}_0) \mathcal{N}(\mathbf{a}_1 | r_i + S_i \mathbf{a}_0, \epsilon S_i), \quad (7)$$



(a) Image-level, L2, Head 57, (b) Object-level, L14, Head 97, (c) Image-level, L17, Head 78, (d) Object-level, L14, Head 113, LLaVA-1.5-7B LLaVA-1.5-7B Qwen2.5-VL-7B Qwen2.5-VL-7B

Fig. 2: A comparison of the hallucination and reliable manifolds in LLaVA-1.5-7B and Qwen2.5-VL-7B is presented through t-SNE visualizations at image and object levels, with transformations between manifolds illustrated via SBP trajectories.

where $\alpha_i(\mathbf{a}_0) = \alpha_i \exp((\mathbf{a}_0^\top S_i \mathbf{a}_0 + 2r_i^\top \mathbf{a}_0)/2\epsilon)$ and $c_\theta(\mathbf{a}_0) = \sum_{i=1}^G \alpha_i(\mathbf{a}_0)$.

We minimize the KL divergence between π^* and π_θ via:

$$\mathcal{L}(\theta) = \mathbb{E}_{\mathbf{a}_0 \sim p_0} [\log c_\theta(\mathbf{a}_0)] - \mathbb{E}_{\mathbf{a}_1 \sim p_1} [\log v_\theta(\mathbf{a}_1)],$$

optimized through mini-batch SGD. This approach enables distribution-level hallucination correction while preserving semantic fidelity and requiring only unpaired hallucination/trustworthy samples.

2.4. Hallucination Mitigation Pipeline for MLLMs

Building on prior theory, as shown in Fig. 1 SchröMind implements a two-stage pipeline. First, we extract attention activations from all Transformer heads (Eq. 1) using both correct and hallucinated VQA pairs. These activations train logistic regression classifiers per head to distinguish hallucinated/factual outputs and enable selection of the top H heads (ranked by classification accuracy) for intervention.

Second, for each selected head, we solve Eq. (2) and Eq. (3) to compute an optimal transport plan and Schrödinger bridge between activation distributions. This dynamically steers unknown tokens’ activations toward factual manifolds:

$$\mathbf{x}^{(k)} = \mathbf{x}^{(k-1)} + \sum_{m=1}^M \left[\mathcal{T}_m^{k-1}(\mathbf{x}^{(k-1)}) \mapsto \mathbf{a}_1|_{m=1}^M \right] \Theta_m^{k-1},$$

where this steering operation maps potentially hallucinated activations $\mathcal{T}_m^{k-1}(\mathbf{x}^{(k-1)})$ to hallucination-resistant distributions $\mathbf{a}_1|_{m=1}^M$ via $\pi_\theta(\mathbf{a}_1 | \mathbf{a}_0)$ (Eq. 7).

The Schrödinger bridge process (Eq. 3) is discretized as:

$$\mathbf{a}_{t+\Delta t} = \mathbf{a}_t + g_\theta(\mathbf{a}_t, t) \Delta t + \sqrt{\epsilon \Delta t} \xi, \quad \xi \sim \mathcal{N}(0, \mathbf{I}), \quad (8)$$

with precomputed drift g_θ guiding activations toward factual outputs. Mitigation strength is controlled by $t \in [0, 1]$, where $t = 0$ (\mathbf{a}_0) implies no intervention and $t = 1$ (\mathbf{a}_1) full intervention.

Interventions occur at two granularities: (1) *image-level* (whole-image perturbations), and (2) *object-level* (object-specific perturbations). When both exist for a head, results are averaged; otherwise, the single applicable intervention is applied. As shown in Fig. 2, the distributions of hallucinated versus factual activations differ significantly across the two visual input settings, necessitating distinct hallucination mitigation trajectories.

3. EXPERIMENTS

3.1. Benchmarks and Evaluation Protocol

Polling-based Object Probing Evaluation (POPE). We evaluate object hallucinations using POPE [17], which employs 27K balanced yes/no queries (half with present/absent objects) from MS COCO [18], A-OKVQA [19], and GQA [20]. Unlike caption-based methods, POPE directly quantifies hallucination tendencies through three sampling strategies (random, popular, adversarial), reporting Accuracy and F1-score.

Multimodal Model Evaluation (MME). MME [21] provides holistic assessment across 14 dimensions: 10 perception tasks (object presence/quantity, spatial relations, color attributes) and 4 cognition tasks (commonsense reasoning (CSR), numerical calculation, text translation, program synthesis), with primary reliance on accuracy metrics.

Experimental Setup. We evaluate SchröMind on LLaVA-1.5-7B [2] and Qwen2.5-VL-7B [22], comparing against VCD [2], OPERA, and ICT [14]¹. Compared to ICT which requires tuning two hyperparameters, our SchröMind relies solely on the top- k attention heads hyperparameter. Following ICT [14], we train logistic regression classifiers on 1,500 activation samples (image/object-level) to identify top- k hallucination-sensitive heads.

3.2. Results and discussion

As shown in Table 1, SchröMind achieves significant performance improvements over both the unmodified regular LLaVA-1.5-7B model and the previous SOTA method ICT across all POPE datasets (MS COCO, A-OKVQA, and GQA). On challenging Adversarial questions, it attains accuracy gains of up to +6.68% (GQA), +5.06% (A-OKVQA), and +6.47% (MS COCO) compared to the regular model. Against ICT, SchröMind leads in 17 out of 18 metrics, with notable improvements in adversarial settings: +3.54% on A-OKVQA and +4.36% on GQA. It is the only method consistently exceeding 80% F1 on Adversarial questions across all datasets, highlighting its enhanced reliability in high-risk scenarios.

¹ICT results reproduced from official implementation: <https://github.com/THU-BPM/ICT>.

Table 1: Performance comparison of SchröMind and baselines on the POPE benchmark using the **LLaVA-1.5-7B** model on three datasets: MSCOCO, A-OKVQA, and GQA. **Bold** and underlined values show the best and second-best, respectively.

Acc.↑/F1↑	MS COCO			A-OKVQA			GQA		
	Random	Popular	Adversarial	Random	Popular	Adversarial	Random	Popular	Adversarial
Regular [2]	83.29/81.33	81.88/80.06	78.96/77.57	83.45/82.56	79.90/79.59	74.04/75.15	83.73/82.95	78.17/78.37	75.08/76.06
VCD [4]	87.73/87.16	85.38/85.06	80.88/81.3	86.15/86.34	81.85/82.82	74.97/77.73	86.65/86.99	80.73/82.24	76.09/78.78
M3ID [11]	86.00/86.00	82.83/83.72	77.70/79.66	83.57/85.09	76.80/80.06	68.10/74.58	82.83/84.62	72.83/77.58	68.13/74.78
OPERA [5]	<u>89.20/88.81</u>	86.64/86.62	81.24/81.38	88.02/84.59	<u>83.22/84.67</u>	73.82/77.91	88.13/88.91	79.27/82.11	75.00/78.71
AVISC [12]	87.93/87.88	84.33/84.96	77.53/79.64	84.60/85.88	78.83/81.63	68.97/75.11	85.00/86.45	74.80/79.17	69.20/75.58
ICT [14]	89.1/88.48	86.76/86.40	83.83/83.84	89.3/89.40	83.4/84.45	<u>75.56/78.68</u>	89.3/89.49	80.86/82.64	77.4/80.11
SchröMind	90.86/89.11	87.1/87.48	85.43/84.48	90.83/90.77	85.63/85.42	79.1/80.15	89.23/89.22	84.83/84.93	81.76/82.31

Table 2: Performance comparison between our SchröMind (SM) and previous SOTA (ICT) on the POPE benchmark using the **Qwen2.5-VL-7B** model across MS COCO, A-OKVQA, and GQA datasets. Results are shown for image-level (w/o obj), object-level (w/o img), and combined interventions. Gray-highlighted entries denote our method.

Acc.↑/F1↑	MS COCO			A-OKVQA			GQA		
	Random	Popular	Adversarial	Random	Popular	Adversarial	Random	Popular	Adversarial
Regular [22]	85.4/82.97	85.13/82.71	84.83/82.42	87.76/86.41	86.43/85.15	81.5/80.78	87.1/85.63	84/82.74	81.6/80.65
ICT w/o obj	86.4/84.31	86.3/84.27	85.7/83.53	89.93/89.15	87.46/86.76	82.5/82.54	88.06/87.01	83.9/83.23	81.63/81.17
SM w/o obj	87.53/85.13	87.33/84.97	87.0/84.62	90.3/89.08	88.56/87.43	83.56/83.04	90.06/88.77	85.3/84.23	82.76/81.97
ICT w/o img	85.4/82.97	85.4/83.07	85.2/82.90	88.76/87.64	86.63/85.50	81.7/81.16	87.16/85.66	83.93/82.67	81.33/80.40
SM w/o img	87.6/85.22	87.26/84.86	87.5/84.72	90.03/88.77	88.4/87.19	83.63/83.05	90.33/89.10	85.36/84.33	82.83/82.12
ICT [14]	87.53/85.84	86.76/84.94	86.16/84.32	88.96/87.90	87.43/86.39	83.6/83.02	88.96/87.89	86.43/85.47	84.1/83.53
SM (ours)	87.93/85.68	87.6/85.33	87.33/86.07	90.66/89.53	88.83/87.80	83.96/83.52	90.3/89.09	87.53/86.52	84.93/84.18

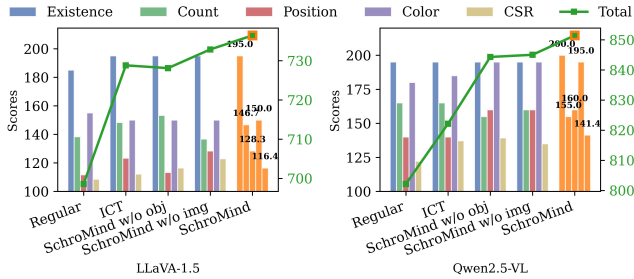


Fig. 3: SchröMind outperforms prior SOTA models (ICT, regular LLaVA-1.5 and Qwen2.5-VL) on MME, with gains in key areas: existence, position, counting, color perception, commonsense reasoning, and overall performance.

Results in Table 2 further confirm these advantages across model architectures. With Qwen2.5-VL-7B, it maintains consistent leads, such as +1.17% on MS COCO and +0.83% on GQA Adversarial, and achieves a new benchmark of 87.53% on GQA Popular. These results establish SchröMind as a universally superior framework for reducing hallucinations.

On the MME benchmark (Fig. 3), SchröMind also outperforms both baseline and ICT methods. With LLaVA-1.5-7B, it reaches a total score of 736.42, exceeding ICT by +7.62 and Regular by +37.85, showing special strength in tasks of *Position* and *Count*. Using Qwen2.5-VL-7B, it sets a new SOTA total score of 851.42, leading in tasks of *Color* (195.0), *Position* (160.0), and *CSR* (141.4).

3.3. Ablation study

To evaluate component contributions in our SchröMind framework, we conducted an ablation study on the POPE benchmark using Qwen2.5-VL-7B. We compared image-level intervention, object-level intervention, and their full integration. As shown in Table 2, both interventions significantly outperform the baseline, with their combination yielding optimal performance. On MS COCO, individual interventions achieve competitive accuracy (87.0–87.6% across subsets), while full SchröMind delivers the strongest results—particularly in all settings. This pattern holds on A-OKVQA (e.g., 90.66% Acc./89.53% F1 on Random) and GQA, where full SchröMind achieves peak performance (90.3% Acc. on Random; 87.53% Acc./86.52% F1 on Popular). Crucially, the synergy between interventions consistently surpasses individual contributions across all datasets and question types, confirming their complementary role in hallucination suppression.

On the MME benchmark (Fig. 3), the full model achieves the highest overall scores (LLaVA-1.5-7B: 736.42; Qwen2.5-VL-7B: 851.42), surpassing ablations by **+3.57–8.33** (LLaVA-1.5-7B) and **+6.42–7.14** (Qwen2.5-VL-7B). The variants show complementary strengths: *w/o image* excels in *Position* and *CSR* but trails in *Count*, while *w/o object* shows the opposite. Only the complete model balances all capabilities, achieving top performance in key subsets such as *Existence* (200.0), *Color* (195.0), and *CSR* (141.42), demonstrating that both intervention types are necessary for robust multimodal reasoning.

4. CONCLUSION

Without increasing computational cost, our proposed SchröMind method provides customized correction for hallucinatory attention activations generated by the Transformer in MLLMs by modeling the transition relationship between hallucinatory and credible attention through dynamic SBP (which is equivalent to static EOT), thereby constructing a correction scheme with the shortest overall migration distance and optimal cost-efficiency. This method effectively corrects attention without compromising the inherent capabilities of MLLMs acquired through extensive training on massive datasets. Experimental results across multiple datasets and benchmarks demonstrate that SchröMind achieves new state-of-the-art performance, significantly outperforming non-customized correction methods.

5. REFERENCES

- [1] Deyao Zhu, Jun Chen, Xiaoqian Shen, Xiang Li, and Mohamed Elhoseiny, “Minigpt-4: Enhancing vision-language understanding with advanced large language models,” *arXiv preprint arXiv:2304.10592*, 2023.
- [2] Haotian Liu, Chunyuan Li, Qingyang Wu, and Yong Jae Lee, “Visual instruction tuning,” *Advances in neural information processing systems*, vol. 36, pp. 34892–34916, 2023.
- [3] Peng Wang, Shuai Bai, Sinan Tan, Shijie Wang, Zhihao Fan, Jinze Bai, Keqin Chen, Xuejing Liu, Jialin Wang, Wenbin Ge, et al., “Qwen2-vl: Enhancing vision-language model’s perception of the world at any resolution,” *arXiv preprint arXiv:2409.12191*, 2024.
- [4] Sicon Leng, Hang Zhang, Guanzheng Chen, Xin Li, Shijian Lu, Chunyan Miao, and Lidong Bing, “Mitigating object hallucinations in large vision-language models through visual contrastive decoding,” in *Proceedings of the IEEE/CVF Conference on Computer Vision and Pattern Recognition*, 2024, pp. 13872–13882.
- [5] Qidong Huang, Xiaoyi Dong, Pan Zhang, Bin Wang, Conghui He, Jiaqi Wang, Dahua Lin, Weiming Zhang, and Nenghai Yu, “Opera: Alleviating hallucination in multi-modal large language models via over-trust penalty and retrospection-allocation,” in *Proceedings of the IEEE/CVF Conference on Computer Vision and Pattern Recognition*, 2024, pp. 13418–13427.
- [6] Hao Yin, Guangzong Si, and Zilei Wang, “Clearsight: Visual signal enhancement for object hallucination mitigation in multimodal large language models,” in *Proceedings of the Computer Vision and Pattern Recognition Conference*, 2025, pp. 14625–14634.
- [7] Chongjun Tu, Peng Ye, Dongzhan Zhou, Lei Bai, Gang Yu, Tao Chen, and Wanli Ouyang, “Attention reallocation: Towards zero-cost and controllable hallucination mitigation of mllms,” *arXiv preprint arXiv:2503.08342*, 2025.
- [8] Ziyu Liu, Yuhang Zang, Xiaoyi Dong, Pan Zhang, Yuhang Cao, Haodong Duan, Conghui He, Yuanjun Xiong, Dahua Lin, and Jiaqi Wang, “Mia-dpo: Multi-image augmented direct preference optimization for large vision-language models,” *arXiv preprint arXiv:2410.17637*, 2024.
- [9] Jinda Lu, Junkang Wu, Jinghan Li, Xiaojun Jia, Shuo Wang, YiFan Zhang, Junfeng Fang, Xiang Wang, and Xiangnan He, “Dama: Data-and model-aware alignment of multi-modal llms,” *arXiv preprint arXiv:2502.01943*, 2025.
- [10] Cong Chen, Mingyu Liu, Chenchen Jing, Yizhou Zhou, Fengyun Rao, Hao Chen, Bo Zhang, and Chunhua Shen, “PerturbollaVA: Reducing multimodal hallucinations with perturbative visual training,” *arXiv preprint arXiv:2503.06486*, 2025.
- [11] Alessandro Favero, Luca Zancato, Matthew Trager, Siddharth Choudhary, Pramuditha Perera, Alessandro Achille, Ashwin Swaminathan, and Stefano Soatto, “Multi-modal hallucination control by visual information grounding,” in *Proceedings of the IEEE/CVF Conference on Computer Vision and Pattern Recognition*, 2024, pp. 14303–14312.
- [12] Sangmin Woo, Donguk Kim, Jaehyuk Jang, Yubin Choi, and Changick Kim, “Don’t miss the forest for the trees: Attentional vision calibration for large vision language models,” *arXiv preprint arXiv:2405.17820*, 2024.
- [13] Kenneth Li, Oam Patel, Fernanda Viégas, Hanspeter Pfister, and Martin Wattenberg, “Inference-time intervention: Eliciting truthful answers from a language model,” *Advances in Neural Information Processing Systems*, vol. 36, pp. 41451–41530, 2023.
- [14] Junzhe Chen, Tianshu Zhang, Shiyu Huang, Yuwei Niu, Linfeng Zhang, Lijie Wen, and Xuming Hu, “Ict: Image-object cross-level trusted intervention for mitigating object hallucination in large vision-language models,” *Proceedings of the IEEE/CVF Conference on Computer Vision and Pattern Recognition*, 2025.
- [15] Christian Léonard, “A survey of the schrödinger problem and some of its connections with optimal transport,” *arXiv preprint arXiv:1308.0215*, 2013.
- [16] Alexander Korotin, Nikita Gushchin, and Evgeny Burnaev, “Light schrödinger bridge,” in *The Twelfth International Conference on Learning Representations*, 2024.
- [17] Yifan Li, Yifan Du, Kun Zhou, Jinpeng Wang, Wayne Xin Zhao, and Ji-Rong Wen, “Evaluating object hallucination in large vision-language models,” *arXiv preprint arXiv:2305.10355*, 2023.
- [18] Tsung-Yi Lin, Michael Maire, Serge Belongie, James Hays, Pietro Perona, Deva Ramanan, Piotr Dollár, and C Lawrence Zitnick, “Microsoft coco: Common objects in context,” in *Computer vision–ECCV 2014: 13th European conference, zurich, Switzerland, September 6–12, 2014, proceedings, part v 13*. Springer, 2014, pp. 740–755.
- [19] Dustin Schwenk, Apoorv Khandelwal, Christopher Clark, Kenneth Marino, and Roozbeh Mottaghi, “A-okvqa: A benchmark for visual question answering using world knowledge,” in *European conference on computer vision*. Springer, 2022, pp. 146–162.
- [20] Drew A Hudson and Christopher D Manning, “Gqa: A new dataset for real-world visual reasoning and compositional question answering,” in *Proceedings of the IEEE/CVF conference on computer vision and pattern recognition*, 2019, pp. 6700–6709.

- [21] Chaoyou Fu, Peixian Chen, Yunhang Shen, Yulei Qin, Meng-dan Zhang, Xu Lin, Jinrui Yang, Xiawu Zheng, Ke Li, Xing Sun, et al., “Mme: A comprehensive evaluation benchmark for multimodal large language models,” *arXiv preprint arXiv:2306.13394*, 2023.
- [22] Shuai Bai, Keqin Chen, Xuejing Liu, Jialin Wang, Wenbin Ge, Sibo Song, Kai Dang, Peng Wang, Shijie Wang, Jun Tang, et al., “Qwen2. 5-vl technical report,” *arXiv preprint arXiv:2502.13923*, 2025.